Subthermocline Tropical Cells and Equatorial Subsurface Countercurrents

By

Chunzai Wang

NOAA Atlantic Oceanographic and Meteorological Laboratory

Miami, Florida

Deep-Sea Research, Part I

August 2004

Corresponding author address: Dr. Chunzai Wang, NOAA/AOML, Physical Oceanography Division, 4301 Rickenbacker Causeway, Miami, FL 33149. E-mail: Chunzai.Wang@noaa.gov.

Abstract

Eastward subsurface countercurrents (SSCCs) are observed in both the Pacific and Atlantic Oceans on either side of the equator, and are associated with a poleward shoaling of subthermocline isotherms at the poleward flanks of the equatorial 13°C thermostad. Observations suggest that eastward SSCCs correspond to a meridional circulation of subthermocline tropical cells (STTCs). The STTCs are below and weaker than the tropical cells, being characterized by an equatorward flow in the thermocline, an equatorial downwelling, a poleward flow in the subthermocline, and an upwelling about 3°-4° from the equator. The essential dynamics of the SSCCs can be explained in terms of the conservation of absolute vorticity in the poleward flow of the lower branch of the STTCs. As a parcel within the subthermocline moves poleward, its gain of planetary vorticity is compensated by a loss of relative vorticity, resulting in the eastward SSCCs. By applying the conservation of potential vorticity, the paper also shows that the poleward shoaling of subthermocline isotherms at the poleward flanks of the thermostad can contribute to the eastward SSCCs.

Keywords: Tropical oceanography; Ocean circulation; Ocean currents; Vorticity; Upwelling; Downwelling.

1. Introduction

A system of surface and subsurface zonal equatorial currents, linked by a meridional circulation driven by Ekman, geostrophic, and non-linear dynamics, has been recognized since the earliest modern observations (e.g., Knauss, 1960, 1966). The equatorial undercurrent (EUC) is continuous along, symmetric about, and tightly confined to the equator with transports comparable to other major ocean currents. Fofonoff and Montgomery (1955) provide the essential dynamics of the EUC in terms of absolute vorticity conservation associated with a meridional circulation of geostrophic equatorward flow in the thermocline (also see Cane, 1980; Philander, 1990). Over most of the equatorial Pacific and Atlantic Oceans, easterly trade winds drive a westward surface flow that produces an eastward pressure gradient force. Meridionally, the surface Ekman flow is poleward while the eastward pressure gradient force induces equatorward geostrophic flow within the thermocline. Equatorial upwelling occurs near the equator and downwelling is located in convergence zones about 3°-4° from the equator. These meridional circulation cells on either side of the equator, recognized a long time ago (e.g., Sverdrup et al., 1942; Defant, 1936), have recently been named the tropical cells (TCs) (e.g., Lu et al., 1998; Johnson et al., 2001; Molinari et al., 2003). Fofonoff and Montgomery (1955) explain that as a parcel moves equatorward associated with the lower branch of the TCs within the thermocline, its loss of planetary vorticity is compensated by a gain of relative vorticity, resulting in the eastward EUC.

The subsurface countercurrents (SSCCs), or Tsuchiya jets, have been observed in both the Pacific and Atlantic Oceans (e.g., Tsuchiya, 1972, 1975; Cochrane et al., 1979; Gouriou and Toole, 1993; Firing et al., 1998; Schott et al., 1998; Rowe et al., 2000; Johnson et al., 2001; Bourles et al., 2002). The persistent eastward subsurface currents are found on either side of the

equator and are associated with subthermocline isotherms plunging toward the equator at the poleward flanks of the 13°C thermostad, a thick layer of nearly homogeneous water near the equatorial region. Several studies have attempted to explain the dynamics of the SSCCs in the Pacific and Atlantic Oceans (McPhaden, 1984; Johnson and Moore, 1997; Marin et al., 2000, 2003; McCreary et al., 2002; Hua et al., 2003; Jochum and Malanotte-Rizzoli, 2004).

The present paper has two major purposes. First, we re-examine and discuss some previously published observational data, and present recent cruise measurements in the western tropical Atlantic Ocean. A combination of different data sets suggests a meridional circulation of subthermocline tropical cells (STTCs) associated with the SSCCs. The STTCs are below and weaker than the TCs, characterized by an equatorward flow in the thermocline, an equatorial downwelling, a poleward flow in the subthermocline, and an upwelling about 3°-4° from the equator. Second, we provide a simple dynamical explanation for the SSCCs in relation to the STTCs, based on the vorticity argument similar to that of Fofonoff and Montgomery (1955) for the EUC.

2. Data

The first data set is from the shipboard Acoustic Doppler Current Profiler (SADCP) data of Johnson et al. (2001). They consider 85 cross-equatorial sections occupied over a nine-year period from 1991 to 1999 in the Pacific Ocean between 170°W and 95°W. Of these 85 cross-equatorial sections, 73 were taken during Tropical Atmosphere-Ocean buoy array maintenance cruises. Seven sections were from World Ocean Circulation Experiment hydrographic cruises and the remaining five sections were from US joint Global Ocean Flux Study Equatorial Pacific

Process Study cruises. These section SADCP data were used to grid zonal and meridional flows [see Johnson et al. (2001) for details].

The second data set is the STC2 (Subtropical Cells 2) cruise data. The STC2 cruise, a joint field program between NOAA/AOML and the University of Kiel, Germany, was carried out in February 2002 for measuring velocity, temperature, salinity, and oxygen in the western tropical Atlantic Ocean. We herein use velocity and temperature measurements of the STC2 cruise along the 35°W meridional section.

The third data set is the ADCP velocity data measured during the Tropical Instability Wave Experiment (TIWE). From May 1990 to June 1991, a diamond-shaped array of five subsurface ADCPs was deployed about 0°, 140°W during the TIWE. Five subsurface moored ADCPs were deployed at 0°, 142°W; 1°S, 140°W; 0°, 138°W; 0°, 140°W; and 1°N, 140°W. This TIWE equatorial array allows to calculate the equatorial vertical velocity component by vertically integrating the continuity equation and by using centered differences for the horizontal divergence (Qiao and Weisberg, 1997; Weisberg and Qiao, 2000; Wang and Weisberg, 2001).

3. Observations of the SSCCs and STTCs

3.1. The SSCCs and poleward shoaling of subthermocline isotherms

The meridional structure of the zonal currents observed in the eastern Pacific Ocean (Johnson et al., 2001) shows the major currents of the equatorial ocean (Fig. 1). Eastward flowing currents include the EUC with a core at 0°, 110 m; the north SSCC with a core at 4°N, 210 m; the south SSCC with a core at 4.5°S, 220 m; and the surface north equatorial countercurrent (NECC) with a core at 7°N, 50 m. Westward flowing currents include the north

branch of the south equatorial current (SEC) with a core at 2°N, 0 m; and the south branch of the SEC with a core at 4°S, 0 m.

The recent STC2 cruise measurements in the tropical Atlantic Ocean along 35°W during February 2002 also show a similar structure of zonal flows. Figure 2a shows all of the important upper ocean currents in the western tropical Atlantic: the EUC, the north SSCC [also called the north equatorial undercurrent (NEUC) in the Atlantic Ocean], the south SSCC [or the south equatorial undercurrent (SEUC)], the North Brazil undercurrent (NBUC), the SEC, and the NECC. The EUC is about 0.5° north of the equator, with maximum eastward flow of about 80 cm s^{-1} at depth of 80-90 m. The SEUC and NEUC, separated from the EUC, flow eastward and are located on either side of the equator at depth of the subthermocline and at latitudes about 3-4° south and north of the equator. Maximum westward flow associated with the NBUC is at depth of 150 m. Both the SEC and the NECC are also evidenced near the surface.

The new cruise measurements in the western tropical Atlantic are also consistent with the classical equatorial dynamical and thermal structure. The temperature of most the EUC water lies in the range 14°-26°C (Figs. 2a and 2b), which implies that the source region for this water is in the subtropics where these isotherms outcrop [Both earlier and recent observations show that the source waters of the Atlantic EUC are dominantly of subtropical South Atlantic origin (e.g., Metcalf and Stalcup, 1967; Schott et al., 1995)]. Water in this temperature range is associated with tongues of high salinity that extend toward the equator, also suggesting that its generation region is the subtropics where evaporation dominates precipitation. The slope of the thermocline, often denoted by the 20°C isotherm in the tropics, is consistent with the distribution of zonal currents (Fig. 2). The NECC coincides with the thermocline slope from the deep trough of the thermocline near 4-5°N to its ridge outside of the data domain. The SEC corresponds to

the thermocline that slopes upward toward the equator. Below the EUC core, the isotherms bow downward, indicating an equatorial downwelling motion. Furthermore, the region below the EUC core, where the vertical shear of zonal current is large, has a very small vertical temperature gradient. Such a subsurface mixed layer, is classically known as thermostad. The south SSCC and north SSCC are at the poleward sides of the thermostad.

The isotherms below the thermocline also show a meridional slope. Figures 2b shows a poleward shoaling of the 10°C-12°C isotherms between 3°-5° off the equator. This poleward slope of the subthermocline is consistent with the geostrophic balance of the eastward south SSCC and north SSCC shown in Fig. 2a. These Atlantic features of cross-equatorial section temperature field measured during February 2002 also appear in the Pacific Ocean observed during the early Hawaii-Tahiti Shuttle Experiment (Wyrtki and Kilonsky, 1984) (Fig. 3). In particular, Figure 3 shows a pronounced shoaling of the 10°C-11°C isotherms near 4°N and 4°S, consistent with the zonal eastward north and south SSCCs of Fig. 1.

3.2. Meridional flows within the subthermocline

A meridional section of the meridional velocity above the thermocline usually manifests the TCs. For example, the meridional structure of the meridional flows observed in the eastern Pacific Ocean (Johnson et al., 2001) shows a classical meridional circulation of the TCs above the thermocline (Fig. 4). Due to the easterly trade winds, the surface flows dominated by Ekman flow are poleward north and south of the equator. At the same time, the easterly trade winds produce an eastward pressure gradient force in the upper ocean that induces equatorward geostrophic flows at depth of the thermocline.

The meridional circulation at depth of the subthermocline was not paid much attention previously. Using the shipboard ADCP data of Johnson et al. (2001), we plotted the meridional section of the meridional velocity (by using contour interval to 1.0 m s^{-1}) to examine the subthermocline meridional circulation in the eastern Pacific. As shown in Fig. 4, the meridional flows at depth of the subthermocline are poleward in both the hemispheres. The poleward flows are asymmetric about the equator, with the northern one vanishing at the latitude of the SSCC core and the flow in the southern hemisphere extended further poleward. The poleward flow in the subthermocline is consistent with the reversed sign of the zonal pressure gradient. The zonal pressure gradient, estimated from hydrographic measurements taken during the Shuttle Experiment, shows that the gradient force reverses sign at about 150-175 m from eastward to westward (see Fig. 3 of McPhaden, 1984). Gouriou and Toole (1993) also demonstrated the reversed sign of the zonal pressure gradient below the thermocline in the equatorial western Pacific Ocean (their Fig. 16), and the numerical model of Hua et al. (2003) simulated the sign reversal (their Fig. 14a). The westward zonal pressure gradient force thus drives geostrophic poleward flow in the subthermocline. The earlier and independent observed data during the Hawaii-Tahiti Shuttle Experiment also showed the poleward flows within the subthermocline (see Fig. 4 of McPhaden, 1984). Thus, the subthermocline poleward flow is a feature of the equatorial circulation although it is smaller than those in the upper layer.

However, we must be cautious of these poleward flows owing to their small amplitude. As Johnson et al. (2001) published their data, they did not discuss the meridional flows in the subthermocline. The reason might be due to that the subthermocline meridional flows are of the same order as the standard error. As shown in Johnson et al. (2001), the thermocline equatorward geostrophic flows (the lower branch of the TCs) are also of the same order as the

standard error. Only do the surface poleward flows largely exceed their standard error. The small subthermocline meridional poleward flows are consistent the small westward zonal pressure gradient in the subthermocline.

3.3. Equatorial downwelling below the EUC core

The small magnitude of vertical velocity (compared to the horizontal velocity) makes direct observations of it difficult. Instead, vertical velocity has been estimated indirectly from observations. We first discuss estimation of vertical velocity from moorings. As mentioned in Section 2, a diamond-shaped array of five subsurface moored ADCPs was deployed about 0°, 140°W in May 1990 for 13 months (Qiao and Weisberg, 1997; Weisberg and Qiao, 2000; Wang and Weisberg, 2001). The array measured horizontal velocity with a high vertical resolution (10 m). The moored observations allowed to calculate the vertical velocity profile at 0°, 140°W by using centered differences for the horizontal divergence and by vertically integrating the continuity equation. The mean vertical velocity profile shows maximum upwelling at 60 m and a zero crossing at 140 m just below the EUC core (Fig. 5). There is a strong downwelling in the lower portion of the EUC with magnitude comparable to that of upwelling above the EUC core. Halpern and Freitag (1987), using moored horizontal current measurements in the eastern equatorial Pacific Ocean, also found a reversal of vertical velocity from upwelling to downwelling. The Atlantic Ocean also shows equatorial downwelling below the EUC core. For example, using a triangular array of four current meter moorings located at about 0°, 28°W, Weingartner and Weisberg (1991) found a reversal from upwelling within and above the EUC core to downwelling over the lower portion of the EUC.

Another approach for estimating vertical velocity is to apply geostrophic and Ekman dynamics to historical hydrography and wind data in a box volume balance (e.g., Wyrtki, 1981; Bryden and Brady, 1985; Meinen et al., 2001). The estimation of Wyrtki (1981) showed upwelling into the surface layer without consideration of vertical velocity below. In a diagnostic study using historical hydrographic data for a box bounded by 5°S-5°N, and 150°W-110°W between the surface and 500 dbar, Bryden and Brady (1985) used geostrophy and Ekman transports to estimate a vertical velocity profile on the equator. Upwelling was found essentially across the entire EUC above the 180 m depth, with relatively small downwelling below. Meinen et al. (2001) estimated vertical velocity from observations of subsurface thermal structure and surface winds over 5°S-5°N, 155°W-95°W during 1993-99. They found equatorial upwelling above about 160 m and equatorial downwelling below.

Equatorial vertical velocity is also estimated by applying the continuity equation to horizontal divergence from the shipboard ADCP sections (e.g., Johnson et al., 2001). Johnson et al. (2001) reported an equatorial vertical velocity that agreed within error bars with Fig. 5. That is, equatorial vertical velocity is upwelling above the thermocline and downwelling below. The difference between the Johnson et al.'s (2001) vertical velocity and Fig. 5 is that the former finds a relatively weaker downwelling below the thermocline.

In summary, all the estimates of equatorial vertical velocity described above show an upwelling above the thermocline and a downwelling below, although the amplitudes of vertical velocity may be different. In addition, the observed upward and downward bowing of the dynamically active and passive tracer isolines (e.g., Knauss, 1966; Wyrtki and Kilonsky, 1984; and Figs. 2b and 3 of this paper) also suggest an upwelling above the thermocline and a downwelling below. It thus seems that equatorial upwelling above the thermocline and

equatorial downwelling below the thermocline (or the EUC core) are a feature of equatorial ocean circulation.

3.4. The subthermocline tropical cells (STTCs)

Observations of meridional flows (e.g., Fig. 4 and others) and equatorial vertical velocity (Fig. 5 and other studies described in the last section) suggest that the tropical upper ocean has double meridional circulation cells: the TCs and STTCs. The schematic diagram of these two cells associated with zonal currents and the atmospheric easterly trade winds is summarized in Fig. 6. The TCs are characterized by a geostrophic equatorward flow in the thermocline, an equatorial upwelling, a surface Ekman poleward flow, a downwelling at about 3°-4° from the equator. The STTCs, below the TCs, are characterized by a geostrophic equatorward flow in the thermocline, an equatorial downwelling, a geostrophic poleward flow in the subthermocline, and an upwelling at about 3°-4° from the equator. The dashed arrows in Fig. 6 indicate that vertical velocity observations is not available to show off-equatorial (about 3°-4° off the equator) downwelling of the TCs and off-equatorial upwelling of the STTCs. However, the downward bowing of the thermocline and the upward bowing of subthermocline isotherms around 3°-4°N (e.g., Figs. 2b and 3) seem to suggest a downwelling above the thermocline and an upwelling below the thermocline, as drawn in the dashed arrows of Fig. 6. The TCs have been extensively studied, especially during the recent years. However, the STTCs have not received much attention in the past even though they are evidenced in different observational data (e.g., McPhaden, 1984; Johnson et al., 2001; Weisberg and Qiao, 2000), probably due to their relatively small amplitude when compared with the surface TCs.

4. A simple explanation for the SSCCs

The essential dynamics of the EUC was first explained by Fofonoff and Montgomery (1955), in terms of the conservation of absolute vorticity in the equatorward flow comprising the lower branch of the meridional TCs (also Cane, 1980; Philander, 1990). Over most of the equatorial Pacific and Atlantic Oceans, easterly winds drive a westward surface flow that produces an eastward pressure gradient force. Meridionally, the surface Ekman flow is poleward while the eastward pressure gradient force induces equatorward geostrophic flow within the thermocline. As a parcel within the thermocline moves equatorward, due to geostrophic convergence, its loss of planetary vorticity is compensated by a gain of relative vorticity, resulting in the eastward EUC.

As detailed in the last section, tropical meridional circulation seems to also display the STTCs in addition to the TCs. Each STTC is associated with a zonal eastward SSCC. The lower branch of the STTC is a poleward geostrophic flow in the subthermocline. We can also apply the vorticity argument to this subthermocline poleward flow. Using observational data, Rowe et al. (2000) calculated the distribution of the potential vorticity and showed that the potential vorticity at both sides of the SSCC core is nearly constant. The conservation of potential vorticity near the equator is:

$$\frac{\beta y - \partial u / \partial y}{h} = \text{constant}, \qquad (1)$$

where β is the planetary vorticity gradient, u is zonal velocity, y is a meridional distance from the equator, and h is a depth of the water column. In Eq. (1), βy is planetary vorticity and

$\partial u/\partial y$ represents relative vorticity. We have neglected the small contribution of the zonal shear of meridional velocity in the relative vorticity of Eq. (1).

First, we discuss the case in that h does not change. If h is constant, Eq. (1) will reduce to the conservation of absolute vorticity:

$$\beta y - \frac{\partial u}{\partial y} = \text{constant}. \tag{2}$$

For a parcel of fluid starting from the initial latitude y_0 that moves poleward, we can integrate Eq. (2) from y_0 to y to obtain:

$$u(y) = \frac{1}{2}\beta(y - y_0)^2 + u(y_0) + u_y(y_0)(y - y_0), \tag{3}$$

where $u(y_0)$ and $u_y(y_0)$ are the zonal current and the shear of the zonal current at the initial latitude y_0, respectively. If we assume that $u(y_0) = 0$ and $u_y(y_0) = 0$ (we do not have to make this assumption), the solution of Eq. (3) can be further simplified to:

$$u(y) = \frac{1}{2}\beta(y - y_0)^2. \tag{4}$$

Equation (4) states that the eastward velocity depends only on the distance between the final and initial latitudes. The larger the distance is, the larger the eastward velocity is. This seems to be consistent with the observation in that, as the SSCCs flow eastward, they diverge from the

equator (the associated STTCs are wide; i.e., $y - y_0$ is large) and their transport increases [see Fig. 11 of Rowe et al. (2000)].

The dominant term in the zonal current solution of Eq. (3) is the first term: $\beta(y - y_0)^2/2$ which is always eastward (positive). That is, no matter where a parcel is starting to move poleward, Eq. (3) gives an eastward flow at depth of the subthermocline regardless of its hemisphere of origin. Physically, as a parcel moves poleward, its gain of planetary vorticity is compensated by a loss of relative vorticity, then resulting in an eastward SSCC flow. Equation (3) shows that the eastward flow also depends upon the zonal current and the shear of the zonal current at the starting latitude. A westward zonal current and a negative shear of the zonal current at y_0 will make the eastward flow less.

Second, we consider the contribution of h. The meridional temperature distribution of Figs. 2b and 3 (also see Fig. 1 of Johnson and Moore, 1997) shows a poleward shoaling of isotherms within the subthermocline near the region of the SSCCs. These observations show that subthermocline isotherms (for example, 10°C or 11°C isotherms) are a nearly linear function of latitude on the equatorial side of the SSCCs. For simplicity, we assume that $h = H - \alpha y$, where H is the depth of a subthermocline isotherm at the equator, and α is a positive constant representing the meridional slope of subthermocline isotherms. (Notice that a more complicated function of h can be used. However, for an analytical solution we herein use a linear function.) If a water column moves poleward from the initial latitude y_0 to y, its potential vorticity is conserved:

$$\frac{\beta y - \partial u/\partial y}{H - \alpha y} = \frac{\beta y_0 - u_y(y_0)}{H_0}, \tag{5}$$

where H_0 is the depth of the subthermocline isotherm at y_0. Integrating Eq. (5) from y_0 to y, we obtain

$$u(y) = \frac{1}{2}\beta(y - y_0)^2 + u(y_0) + u_y(y_0)(y - y_0) + \frac{\alpha}{2H}[\beta y_0 - u_y(y_0)](y^2 - y_0^2). \qquad (6)$$

In the derivation of Eq. (6), we have used $H_0 \approx H$ for simplicity. Comparison of Eq. (6) with Eq. (3) shows that the last term in Eq. (6) represents the contribution of the poleward shoaling of subthermocline isotherms to the eastward SSCC. Since α and $y^2 - y_0^2$ are always positive (associated with a poleward movement) and $\beta y_0 - u_y(y_0)$ is positive below the EUC core, the poleward slope of isotherms in the subthermocline contributes to an eastward flow. Physically, as a water column moves poleward, its layer thickness decreases (e.g., Figs. 2b and 3) and conservation of potential vorticity requires a decrease in relative vorticity that contributes to the eastward SSCCs. The potential vorticity argument herein is consistent with the recent observation of Rowe et al. (2000) who showed that the potential vorticity of the north and south sides of the SSCCs is nearly constant.

5. Discussion and Summary

The eastward SSCCs are observed in both the Pacific and Atlantic Oceans on either side of the equator, and are associated with the poleward shoaling of subthermocline isotherms at the poleward flanks of the equatorial 13°C thermostad. Observations suggest that the eastward SSCCs correspond to the subthermocline meridional circulation of the STTCs. The STTCs, below and weaker than the TCs, are characterized by an equatorward flow in the thermocline, an equatorial downwelling, a poleward flow in the subthermocline, and an upwelling about 3°-4°

from the equator. The existence of the STTCs is consistent with the observed westward zonal pressure gradient that drives the poleward geostrophic flow in the subthermocline. The equatorial downwelling below the thermocline of the STTCs may be supplied by the equatorward geostrophic convergent flow observed in the thermocline depth, and may be a result of the poleward geostrophic divergence in the subthermocline.

The essential dynamics of the SSCCs can be explained in terms of the conservation of absolute vorticity in the poleward geostrophic flow of the lower branch of the STTCs. As a parcel within the subthermocline moves poleward, its gain of planetary vorticity is compensated by a loss of relative vorticity, resulting in the eastward SSCCs. By applying the conservation of potential vorticity, we also show that the poleward shoaling of subthermocline isotherms at the poleward flanks of the thermostad can contribute to the SSCCs. The vorticity arguments for the SSCCs herein are consistent with the recent observation of Rowe et al. (2000). Rowe et al. (2000) observed that, when approached from the equatorward side of the SSCCs to the SSCC core, an increase in planetary vorticity is companied with a decrease in relative vorticity. They also showed that the potential vorticity of the equatorward side of the SSCCs is nearly constant [also see the numerical modeling results of Hua et al. (2003) and Marin et al. (2003)].

The vorticity arguments for the existence of the EUC (Fofonoff and Montgomery, 1955; Cane, 1980; Philander, 1990) and the SSCCs have similarities and dissimilarities. A zonal eastward jet-like flow has a positive and negative relative vorticity in the north and south sides of the jet core, respectively. For the EUC, a parcel is moved equatorward in the thermocline. A loss of planetary vorticity is compensated by an increase in the relative vorticity, then causing an eastward EUC near the equator. On the other hand, the SSCCs correspond to a poleward flow in the subthermocline. A poleward-moving parcel increases its planetary vorticity, compensated by

a decrease in the relative vorticity, resulting in an eastward SSCC in the region of 3°-4° from the equator. Like the EUC, the vorticity argument for the SSCC applies to both the hemispheres due to the change of sign of the Coriolis parameter.

In the literature, several studies have attempted to explain dynamics of the SSCCs. McPhaden (1984) explored the SSCCs by using a linear, vertically diffusive, and steady model. In his model, the SSCCs are driven by the cyclonic vorticity of the EUC. The cyclonic vorticity in the EUC diffuses downward into the deeper ocean where it is balanced by advection of planetary vorticity. Away from the diffusive boundary layer, the planetary vorticity advection is balanced by vortex stretching that weakens the temperature stratification: a thermostad is then formed and the SSCC appears as the geostrophic response to this thermostad. His model result showed that the SSCC appears as downward-bending lobes attached to the EUC, consistent with the SSCCs observed in the western Pacific (e.g., Johnson et al., 2002). However, the model result is inconsistent with the SSCCs in the eastern and central part of ocean basins where the SSCCs are observed to be distinctly separated from the EUC. Nevertheless, McPhaden's (1984) model results showed a meridional poleward flow below the thermocline associated with a reversed sign of zonal pressure gradient below 200 m. These are consistent with the observed meridional circulation of the STTCs reported in this paper.

Johnson and Moore (1997) sought to explain the observation that the SSCCs diverge from the equator as they flow eastward, employing an inertial jet model based on the conservation of both Bernouli function and potential vorticity. They specified an initial eastward jet-like flow in the western Pacific and a west-east slope of the pycnoline. Their model solution is determined by the initially specified eastward jet-like flow in the western Pacific and the zonal slope of the pycnocline. As a jet flows eastward, the simulated SSCC shifts poleward as a result

of the conservation of Bernouli function and potential vorticity due to the specified pycnocline thickness. However, this model could not address the mechanism that initially creates the eastward SSCCs.

Marin et al. (2000) used a two-dimensional model to explain the existence of the SSCCs with a specified density distribution. Their model produces an eastward SSCC and an ageostrophic secondary meridional circulation cell below the thermocline. They argued that ageostrophic poleward flows below the pycnocline carry near-equatorial water parcels poleward. The parcels conserve their angular momentum and consequently produce eastward jets near 3°N (S). Although their model results seem to support the meridional circulation of the STTCs reported herein, the STTCs are observed for total (including geostrophic) flows in the meridional section rather than ageostrophic secondary flows as produced in the Marin et al. (2000) model. Recently, Hua et al. (2003) and Marin et al. (2003) employed a fully three-dimensional model to support the results of their two-dimensional model.

Based on the results of highly idealized layer models, McCreary et al. (2002) concluded that the existence of the Pacific SSCCs is due to the Indonesian Throughflow. They noted that the Atlantic meridional overturning circulation (MOC) may play an analogous role to the Indonesian Throughflow and can drive the Atlantic SSCCs. A numerical general circulation model by Jochum and Malanotte-Rizzoli (2004) showed that the MOC can not produce the SSCCs in the Atlantic Ocean. Jochum and Malanotte-Rizzoli (2004) claimed that the tropical instability wave (TIW) is a source of eddy heat and momentum fluxes that maintain the SSCCs. However, their model may be difficult to explain the existence of the SSCCs in the western part of ocean basins, since the TIW is mostly observed in the eastern part of ocean basins.

Our simple explanation for the SSCCs, based on the vorticity arguments in relation to the STTCs, is not necessarily in contradiction with the SSCC mechanisms discussed above. In contrast, some of these studies are consistent with and support the results reported in this paper. We regard the vorticity argument for explaining the SSCCs as very simple but fundamental, like the classical explanation of the EUC. However, the model herein as it stands is very simple, making it unsuitable to use for quantitative diagnosis. Although the model produces an eastward subthermocline flow, it is not expected to explain all aspects of the SSCCs. For a perfect meridional STTC cell as shown in Fig. 6, the meridional velocity should vanish at the latitude of the SSCC core where the vertical velocity is expected to be maximum. It is indeed the case in the northern hemisphere that shows a zero subthermocline meridional flow around the SSCC core at 3-4°N (Fig. 4). However, it is not true in the southern hemisphere. This asymmetry, along with why the south SSCC is also located at 3-4°S, deserves a further study.

The results presented in this paper may not apply to the western Pacific. To my knowledge, equatorial downwelling below the EUC is not observed in the western Pacific Ocean. In contrast, Helber and Weisberg (2001) reported an equatorial upwelling at 156°E. As shown in Johnson et al. (2002), the SSCCs in the western Pacific are not separated from the EUC. The diffusive model of McPhaden (1984) showed that the SSCCs are driven by the cyclonic vorticity of the EUC diffused downward and they appear as a lobe attached to the EUC. It is possible that the diffusive term plays an important role in western Pacific SSCCs and vorticity does not conserve there.

The subthermocline meridional circulation of the STTCs has appeared in the earlier observational data. However, it was not emphasized and their importance was not recognized, probably due to their relatively small amplitude in comparison with that of the TCs. Although

the small poleward flow in the subthermocline is consistent with the small westward zonal pressure gradient force, Johnson et al. (2001) showed that the poleward flow is observed to be of the same order as standard error (it is also true for the thermocline equatorward flow of the TCs). We thus caution that the results in this paper are only suggestive, but not conclusive. We hope that the present paper will stimulate more studies of the SSCCs and STTCs, in particular, by numerical models.

Acknowledgments. This work was supported by a grant from NOAA Office of Global Programs and by NOAA Environmental Research Laboratories through their base funding of Atlantic Oceanographic and Meteorological Laboratory (AOML). I thank G. Johnson, R. Molinari, F. Schott, and R. Weisberg for providing observational data used in this paper. D. Snowden and X. Xia assisted in some figures presented in this paper. Comments by C. Meinen, G. Johnson, R. Molinari, F. Ascani, and anonymous reviewers helped improve the paper.

References

Arthur, R. S., 1960. A review of the calculation of ocean currents at the equator. Deep-Sea Research 6, 287-297.

Bourles, B., D'Orgeville, M., Eldin, G., Gouriou, Y., Chuchla, R., DuPenhoat, Y., Arnault, S., 2002. On the evolution of the thermocline and subthermocline eastward currents in the equatorial Atlantic. Geophysical Research Letters 29, 10.1029/2002GL015098.

Bryden, H. L., Brady, E. C., 1985. Diagnostic model of the three-dimensional circulation in the upper equatorial Pacific Ocean. Journal Physical Oceanography 15, 1255-1273.

Cane, M. A., 1980. On the dynamics of equatorial currents with application to the Indian Ocean. Deep-Sea Research 27A, 525-544.

Cochrane, J. D., Kelly, F. J., Olling, C. R., 1979. Subthermocline contercurrents in the western equatorial Atlantic Ocean. Journal of Physical Oceanography 9, 724-738.

Defant, A., 1936. Die Troposphere. Deutsche Atalantishe Exped. Meteor. 6, 289-411.

Firing, E., Wijffels, S. E., Hacker, P., 1998. Equatorial subthermocline currents across the Pacific. Journal of Geophysical Research 103, 21,413-21,423.

Fofonoff, N. P., Montgomery, R. B., 1955. The Equatorial Undercurrent in the light of the vorticity equation. Tellus 7, 518-521.

Gouriou, Y., Toole, J., 1993. Mean circulation of the upper layers of the western equatorial Pacific Ocean. Journal of Geophysical Research 98 (C12), 22495-22520.

Halpern, D., Freitag, H. P., 1987. Vertical motion in the upper ocean of the equatorial eastern Pacific. Oceanologica Acta 6, 19-26.

Helber, R. W., Weisberg, R. H., 2001. Equatorial upwelling in the western Pacific warm pool. Journal of Geophysical Research 106, 8989-9003.

Hua, B. L., Marin, F., Schopp, R., 2003. Three-dimensional dynamics of the subsurface countercurrents and equatorial thermostad. Part I: Formulation of the problem and generic properties. Journal of Physical Oceanography 33, 2588-2609.

Jochum, M., Malanotte-Rizzoli, P., 2004. A new theory for the generation of the equatorial subsurface countercurrents. Journal of Physical Oceanography 34, 755-771.

Johnson, G. C., Moore, D. W., 1997. The Pacific subsurface countercurrents and an inertial model. Journal of Physical Oceanography 27, 2448-2459.

Johnson, G. C., McPhaden, M. J., Firing, E., 2001. Equatorial Pacific Ocean horizontal velocity, divergence and upwelling. Journal of Physical Oceanography 31, 839-849.

Johnson, G. C., Sloyan, B. M., Kessler, W. S., McTaggart, K. E., 2002. Direct measurements of upper ocean currents and water properties across the tropical Pacific during the 1990s. Progress in Oceanography 52, 31-61.

Knauss, J. A., 1960. Measurements of the Cromwell Current. Deep-Sea Research 6, 265-286.

Knauss, J. A., 1966. Further measurements and observations of the Cromwell Current. Journal of Marine Research 24, 205-240.

Lu, P., McCreary, J. P., Klinger, B. A., 1998. Meridional circulation cells and the source waters of the Pacific equatorial undercurrent. Journal of Physical Oceanography 28, 62-84.

Marin, F., Hua, B. L., Wacongne, S., 2000. The equatorial thermostad and subsurface countercurrents in the light of the dynamics of atmospheric Hadley cells. Journal of Marine Research 58, 405-437.

Marin, F., Schopp, R., Hua, B. L., 2003. Three-dimensional dynamics of the subsurface countercurrents and equatorial thermostad. Part II: Influence of the large-scale ventilation and equatorial winds. Journal of Physical Oceanography 33, 2610-2626.

McCreary, J. P., Lu, P., Yu, Z., 2002. Dynamics of the Pacific subsurface countercurrents. Journal of Physical Oceanography 32, 2379-2404.

McPhaden, M. J., 1984. On the dynamics of equatorial subsurface countercurrents. Journal of Physical Oceanography 14, 1216-1225.

Meinen, C. S., McPhaden, M. J., Johnson, G. C., 2001. Vertical velocities and transports in the equatorial Pacific during 1993-99. Journal of Physical Oceanography 31, 3230-3248.

Metcalf, W. G., Stalcup, M. C., 1967. Origin of the Atlantic equatorial undercurrent. Journal of Geophysical Research 72, 4959-4975.

Molinari, R. L., Bauer, S., Snowden, D., Johnson, G. C., Bourles, B., Gouriou, Y., Mercier, H., 2003. A comparison of kinematic evidence for tropical cells in the Atlantic and Pacific Oceans. In: Goni, G, Malanotte-Rizzoli, P. (Eds.), *Interhemispheric Water Exchange in the Atlantic Ocean*. Elsevier Oceanography Series, pp. 269-286.

Philander, S. G., 1990. *El Niño, La Niña, and the Southern Oscillation*. Academic Press, London, 289 pp.

Qiao, L., Weisberg, R. H., 1997. The zonal momentum balance of the Equatorial Undercurrent in the central Pacific. Journal of Physical Oceanography 27, 1094-1119.

Rowe, G. D., Firing, E., Johnson, G. C., 2000. Pacific equatorial subsurface countercurrent velocity, tranport, and potential vorticity. Journal of Physical Oceanography 30, 1172-1187.

Schott, F. A., Stramma, L., Fischer, J., 1995. The warm water inflow into the western tropical Atlantic boundary regime, spring 1994. Journal of Geophysical Research 100, 24745-24760.

Schott, F. A., Fischer, J., Stramma, L., 1998. Transports and pathways of the upper-layer circulation in the western tropical Atlantic. Journal of Physical Oceanography 28, 1904-1928.

Sverdrup, H. U., Johnson, M. W., Fleming, R. H., 1942. *The oceans, Physics, Chemistry and General Biology*. Prentice-Hall, 1087 pp.

Tsuchiya, M., 1972. A subsurface north equatorial countercurrent in the eastern Pacific Ocean. Journal of Geophysical Research 77, 5981-5986.

Tsuchiya, M., 1975. Subsurface Countercurrents in the eastern equatorial Pacific Ocean. Journal of Marine Research 33, 125-175.

Wang, C., Weisberg, R. H., 2001. Ocean circulation influences on SST in the equatorial central Pacific. Journal of Geophysical Research 106, 19515-19526.

Weingartner, T. J., Weisberg, R. H., 1991. On the annual cycle of equatorial upwelling in the central Atlantic Ocean. Journal of Physical Oceanography 21, 68-82.

Weisberg, R. H., Qiao, L., 2000. Equatorial upwelling in the central Pacific estimated from moored velocity profilers. Journal of Physical Oceanography 30, 105-124.

Wyrtki, K., 1981. An estimate of equatorial upwelling in the Pacific. Journal of Physical Oceanography 11, 1205-1214.

Wyrtki, K, Kilonsky, B., 1984. Mean water and current structure during the Hawaii-to-Tahiti Shuttle Experiment. Journal of Physical Oceanography 14, 242-254.

Figure Captions

Figure 1. Observations of zonal velocity (cm/s) in the eastern Pacific Ocean (136°W). Shown are the equatorial undercurrent (EUC), the north subsurface countercurrent (SSCC), the south SSCC, the north equatorial countercurrent (NECC), the north branch of the south equatorial current (SEC), and the south branch of the SEC. Eastward (positive) velocity is shaded. The figure is redrawn from the shipboard ADCP data of Johnson et al. (2001).

Figure 2. Shipboard ADCP and CTD measurements of (a) zonal velocity (cm/s) and (b) temperature (°C) in the western Atlantic Ocean at 35°W in February 2002. Zonal currents include the equatorial undercurrent (EUC), the north subsurface countercurrent (SSCC) [also called north equatorial undercurrent (NEUC) in the Atlantic], the south SSCC [or south equatorial undercurrent (SEUC)], the North Brazil undercurrent (NBUC), the south equatorial current (SEC), and the north equatorial countercurrent (NECC). Eastward (positive) velocity is shaded.

Figure 3. Meridional section of mean temperature (°C) as a function of depth and latitude from the Hawaii-Tahiti Shuttle Experiment (Wyrtki and Kilonsky, 1984).

Figure 4. Observations of meridional velocity (cm/s) in the Pacific Ocean around 136°W. The surface Ekman flow is poleward while the geostrophic flow in the thermocline is equatorward. In the subthermocline, the geostrophic flow poleward. Arrows are drawn showing the directions of meridional flows at different depths. Northward (positive) velocity is shaded. The figure is

redrawn from the shipboard ADCP data of Johnson et al. (2001) by increasing contour interval to 1.0 m/s to emphasize the subthermocline meridional flow.

Figure 5. Observations of the vertical distribution of equatorial vertical velocity (10^{-3} cm/s) at 0°, 140°W from the TIWE array. The TIWE array includes five subsurface moored ADCPs at 0°, 142°W; 1°S, 140°W; 0°, 138°W; 0°, 140°W; and 1°N, 140°W. The equatorial vertical velocity was calculated by using centered differences for the horizontal divergence and by vertically integrating the continuity equation. Arrows are drawn showing equatorial upwelling and downwelling.

Figure 6. Schematic diagram of equatorial ocean circulation in response to the easterly trade wind. Zonal currents include the equatorial undercurrent (EUC), the subsurface countercurrents (SSCCs), and the south equatorial current (SEC). Meridional circulation shows double cells: the tropical cells (TCs) and the subthermocline tropical cells (STTCs). The symbols of × and • represent flows in and out of paper, respectively.

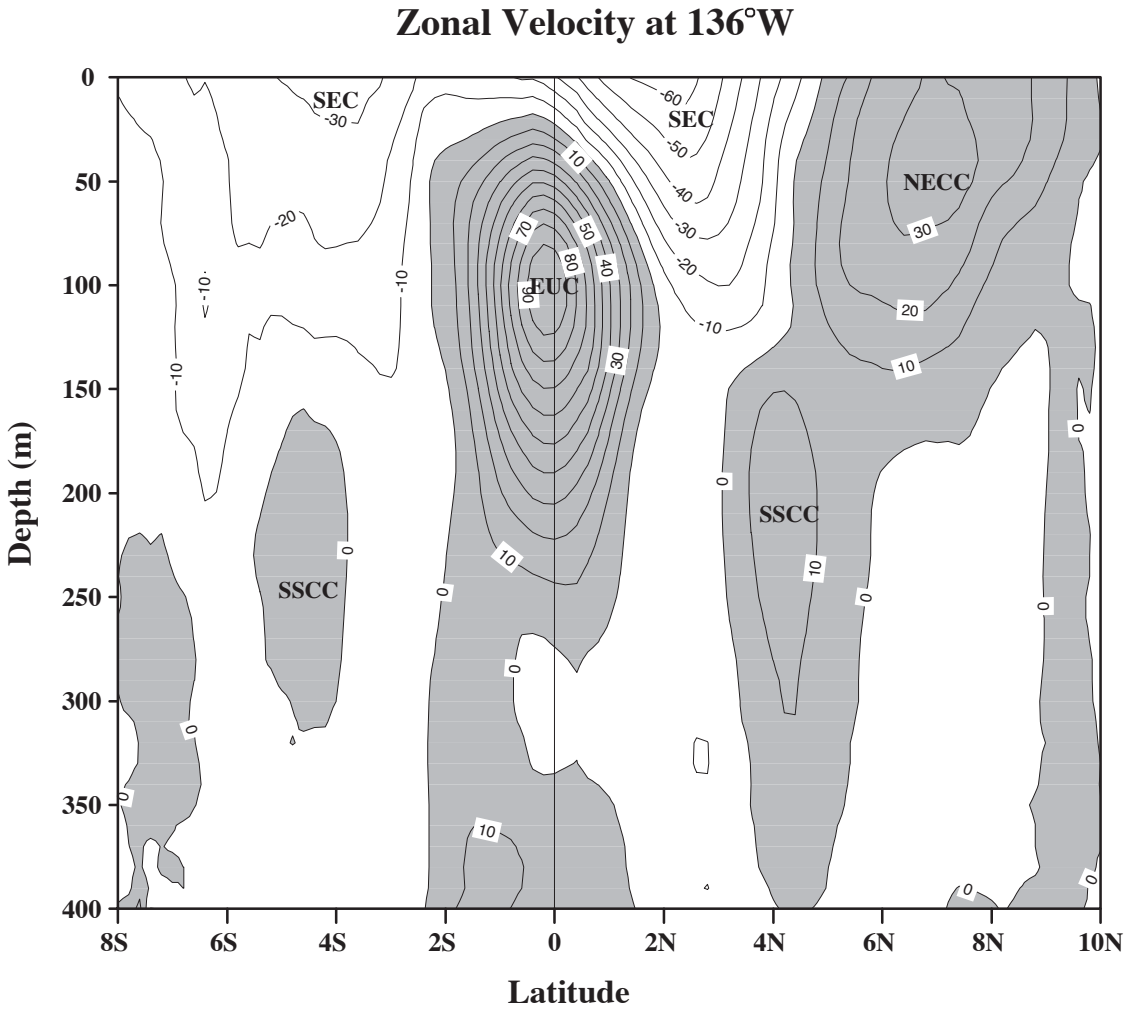

Figure 1. Observations of zonal velocity (cm/s) in the eastern Pacific Ocean (136°W). Shown are the equatorial undercurrent (EUC), the north subsurface countercurrent (SSCC), the south SSCC, the north equatorial countercurrent (NECC), the north branch of the south equatorial current (SEC), and the south branch of the SEC. Eastward (positive) velocity is shaded. The figure is redrawn from the shipboard ADCP data of Johnson et al. (2001).

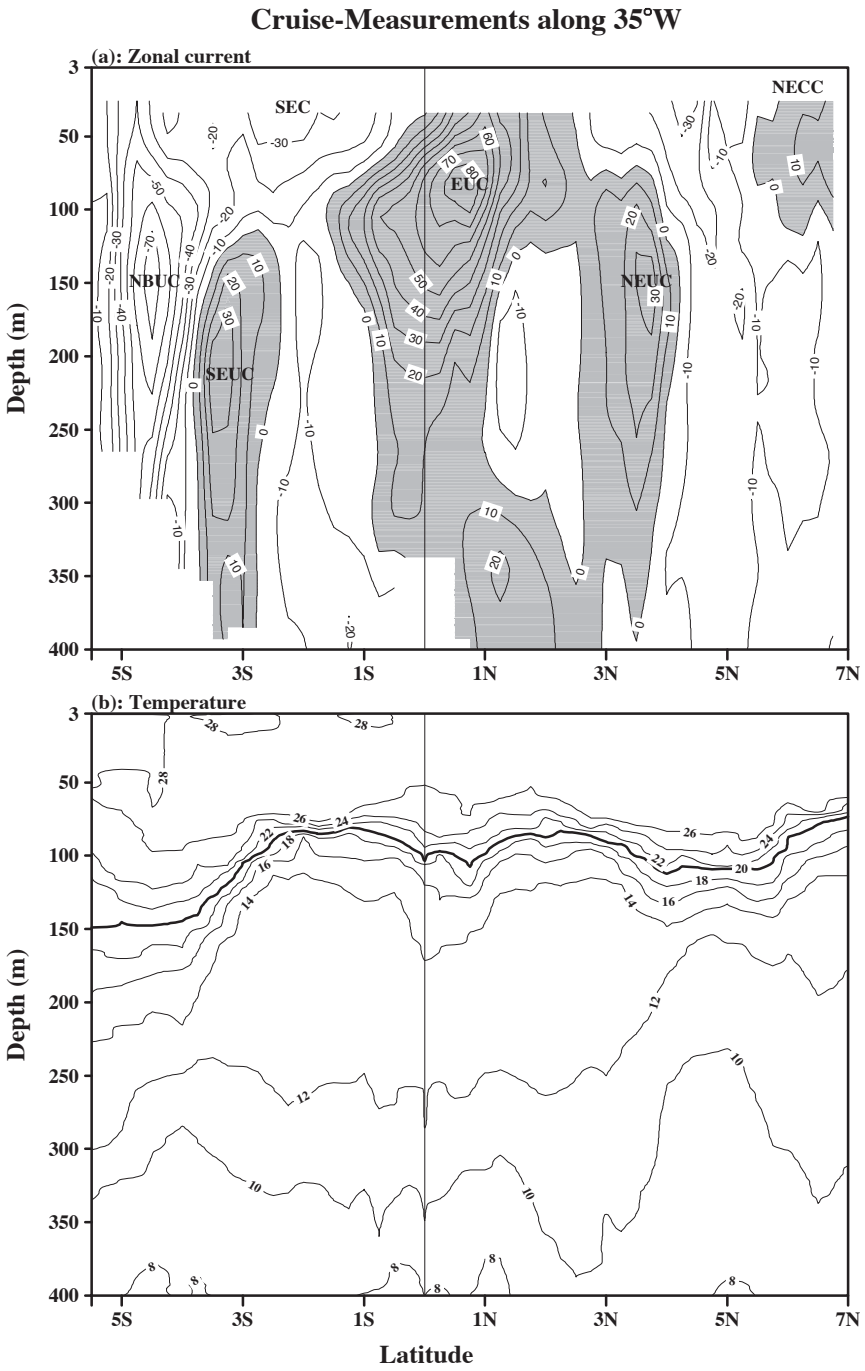

Figure 2. Shipboard ADCP and CTD measurements of (a) zonal velocity (cm/s) and (b) temperature (°C) in the western Atlantic Ocean at 35°W in February 2002. Zonal currents include the equatorial undercurrent (EUC), the north subsurface countercurrent (SSCC) [also called north equatorial undercurrent (NEUC) in the Atlantic], the south SSCC [or south equatorial undercurrent (SEUC)], the North Brazil undercurrent (NBUC), the south equatorial current (SEC), and the north equatorial countercurrent (NECC). Eastward (positive) velocity is shaded.

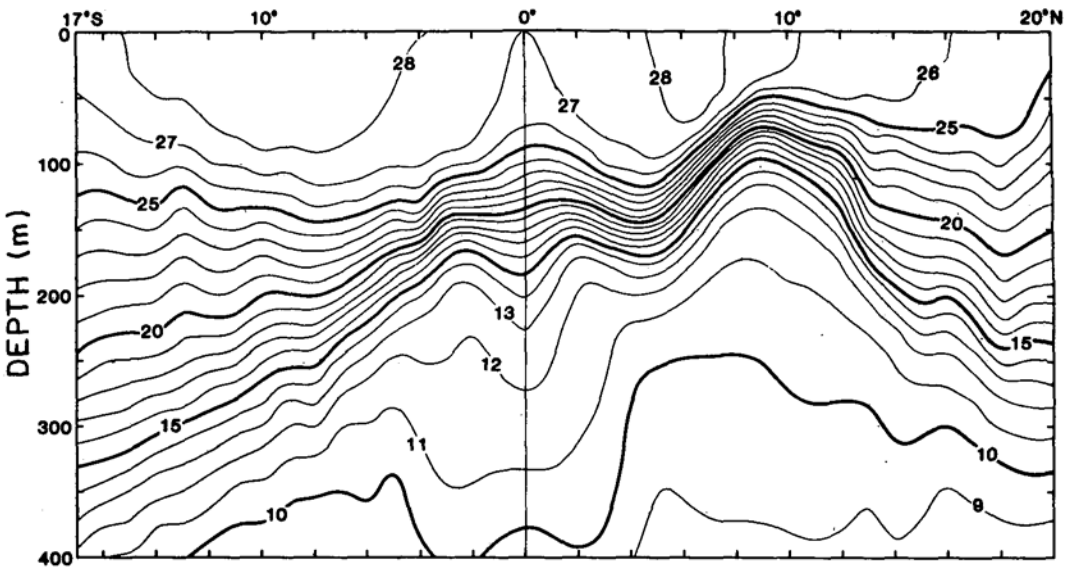

Figure 3. Meridional section of mean temperature (°C) as a function of depth and latitude from the Hawaii-Tahiti Shuttle Experiment (Wyrtki and Kilonsky, 1984).

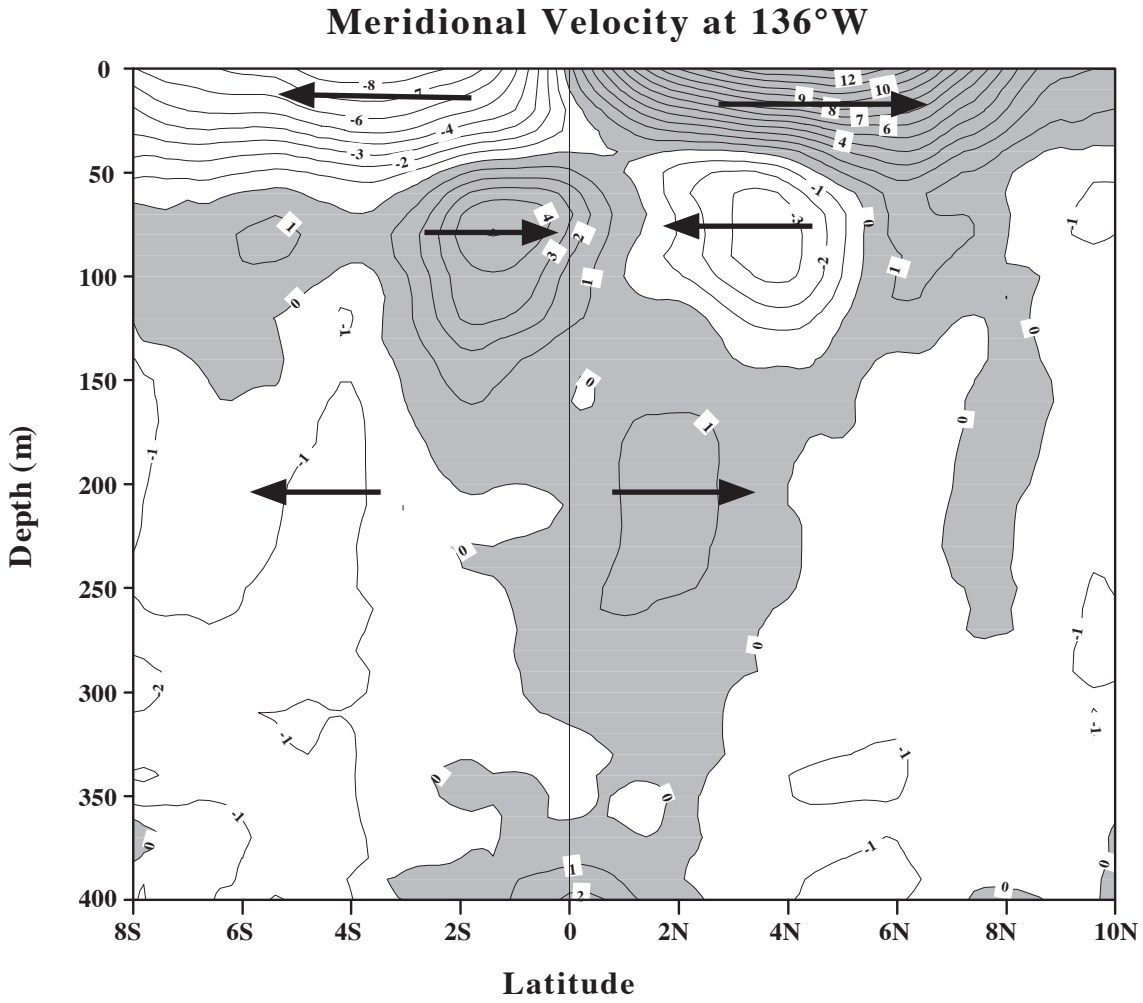

Figure 4. Observations of meridional velocity (cm/s) in the Pacific Ocean around 136°W. The surface Ekman flow is poleward while the geostrophic flow in the thermocline is equatorward. In the subthermocline, the geostrophic flow poleward. Arrows are drawn showing the directions of meridional flows at different depths. Northward (positive) velocity is shaded. The figure is redrawn from the shipboard ADCP data of Johnson et al. (2001) by increasing contour interval to 1.0 m/s to emphasize the subthermocline meridional flow.

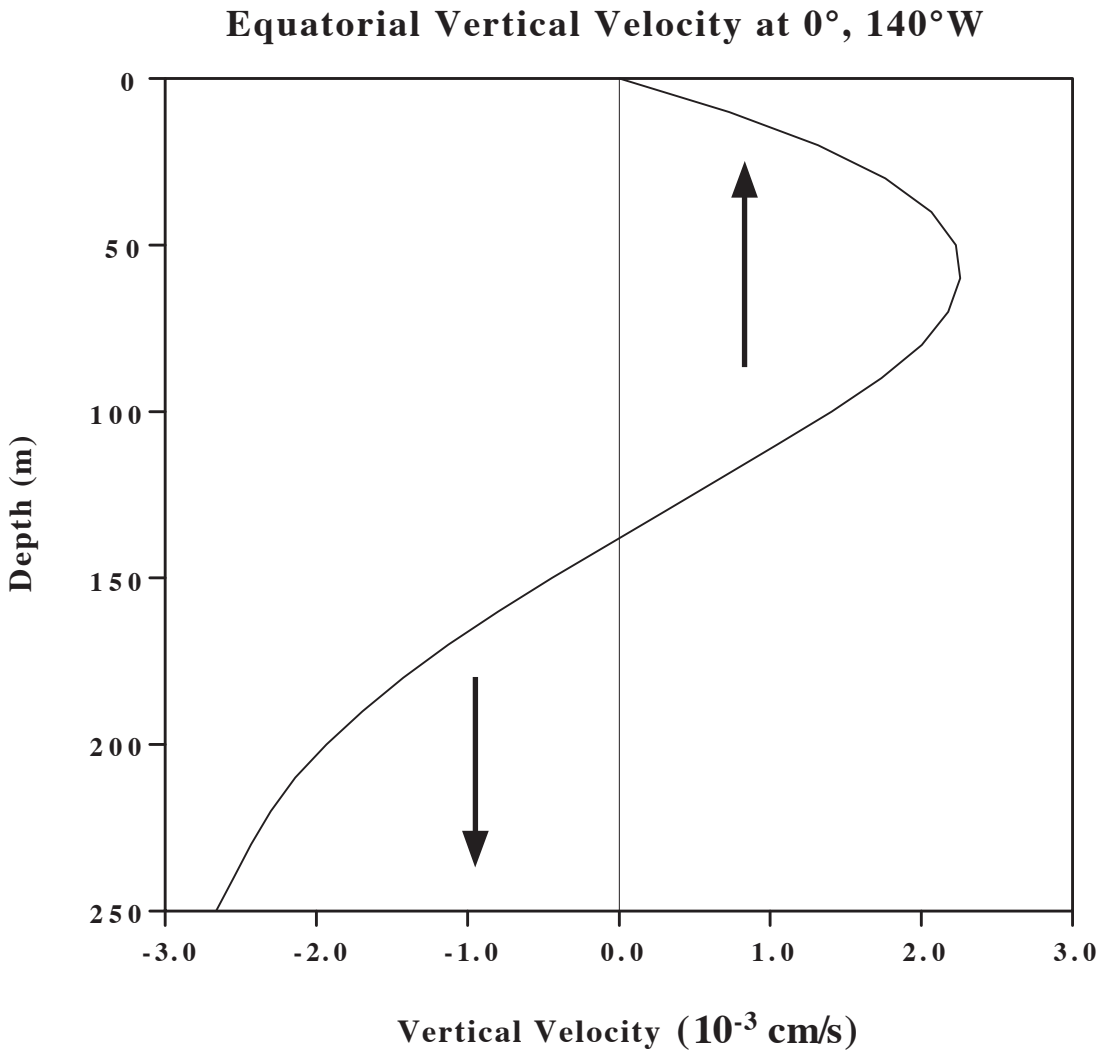

Figure 5. Observations of the vertical distribution of equatorial vertical velocity (10^{-3} cm/s) at 0°, 140°W from the TIWE array. The TIWE array includes five subsurface moored ADCPs at 0°, 142°W; 1°S, 140°W; 0°, 138°W; 0°, 140°W; and 1°N, 140°W. The equatorial vertical velocity was calculated by using centered differences for the horizontal divergence and by vertically integrating the continuity equation. Arrows are drawn showing equatorial upwelling and downwelling.

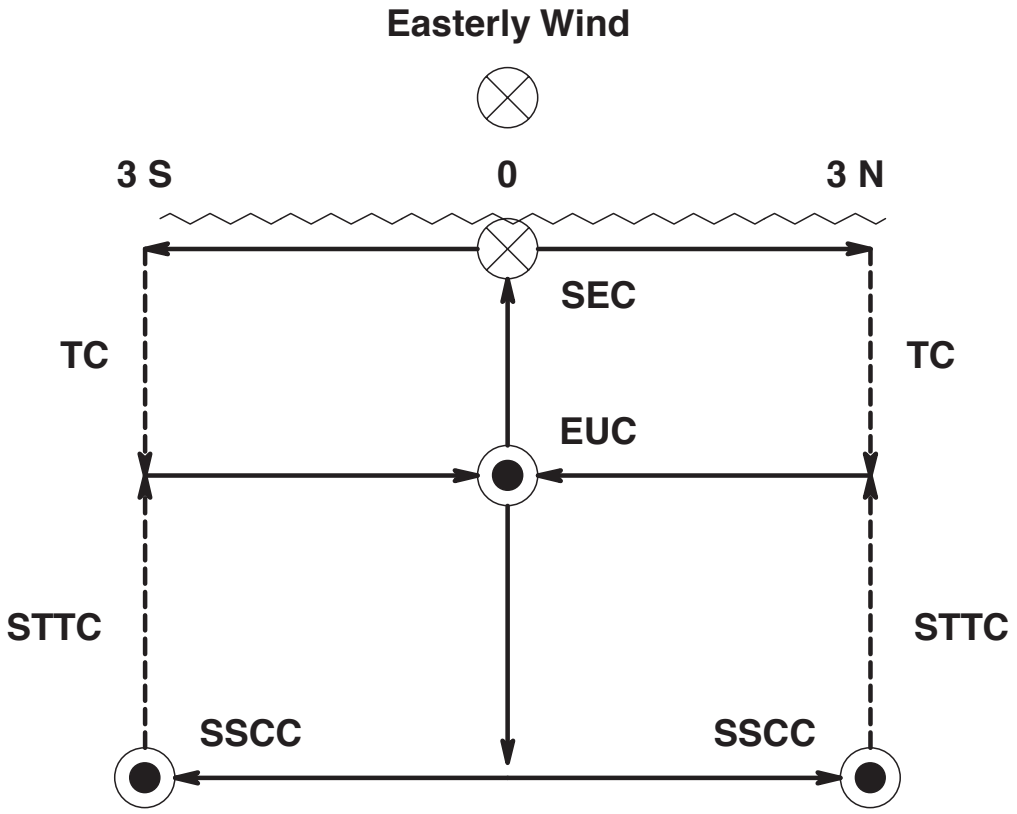

Figure 6. Schematic diagram of equatorial ocean circulation in response to the easterly trade wind. Zonal currents include the equatorial undercurrent (EUC), the subsurface countercurrents (SSCCs), and the south equatorial current (SEC). Meridional circulation shows double cells: the tropical cells (TCs) and the subthermocline tropical cells (STTCs). The symbols of × and • represent flows in and out of paper, respectively.